Hindawi Publishing Corporation
Advances in Astronomy
Volume 2010, Article ID 184284, 14 pages
doi:10.1155/2010/184284

Review Article

Constraints on the Dark Side of the Universe and Observational Hubble Parameter Data

Tong-Jie Zhang,[1,2] Cong Ma,[1] and Tian Lan[1]

[1] *Department of Astronomy, Beijing Normal University, Beijing 100875, China*
[2] *Center for High Energy Physics, Peking University, Beijing 100871, China*

Correspondence should be addressed to Tong-Jie Zhang, tjzhang@bnu.edu.cn

Received 2 August 2010; Revised 24 November 2010; Accepted 13 December 2010

Academic Editor: Gary Wegner

This paper is a review on the observational Hubble parameter data that have gained increasing attention in recent years for their illuminating power on the dark side of the universe: the dark matter, dark energy, and the dark age. Currently, there are two major methods of independent observational $H(z)$ measurement, which we summarize as the "differential age method" and the "radial BAO size method." Starting with fundamental cosmological notions such as the spacetime coordinates in an expanding universe, we present the basic principles behind the two methods. We further review the two methods in greater detail, including the source of errors. We show how the observational $H(z)$ data present itself as a useful tool in the study of cosmological models and parameter constraint, and we also discuss several issues associated with their applications. Finally, we point the reader to a future prospect of upcoming observation programs that will lead to some major improvements in the quality of observational $H(z)$ data.

1. Introduction

The expansion of our universe has been one of the greatest attractions of scientific talents since the seminal work of Edwin Powell Hubble [1] in 1929. Hubble's compilation of observational distance-redshift (expressed in terms of radial velocity) data suggested a linear pattern of "extra-Galactic nebulae" (an archaic term for galaxies) receding from each other

$$\dot{\mathbf{x}} = H\mathbf{x}, \tag{1}$$

where H is the proportional constant now bearing his name, and x is the positional coordinates of a galaxy measured with our Galaxy as the origin.

The discovery of Hubble's Law marked the commencement of the era of quantitative cosmology in which theories of the universe can be subjected to observational test. Since the days of Hubble, advances in technology have enabled astronomers to measure the light from increasingly deeper space and more ancient time and our ideas of the entire history of the expanding universe have been gradually converging into a unified picture of the Big Bang-Cold Dark Matter universe. In this picture, the dominating form of energy density transited from radiation to dark matter, and relics of primordial perturbation were imprinted on today's observable CMB anisotropy and large-scale structures (LSS). This picture is obtained from its two ends: the CMB last-scattering surface at $z \approx 1000$ and the LSS around us at $z \approx 0$. The vast spacetime extent between both ends, in particular the era before reionization, remains mostly hidden from our view. In addition, the past two decades' cosmological observations, especially those of type Ia supernovae (SNIa), indicated that the recent history of universal expansion is an acceleration, possibly driven by an unknown "dark energy" [2, 3] whose physical nature has not been identified.

Therefore, it appears to us that our understanding of the universe is currently under the shade of three dark clouds: the mysterious *dark energy* that drives late-time accelerated expansion, the nature of *dark matter* that is vital to the formation of structures, and the unfathomable *dark age* that has not yet revealed itself to observations. This is the "3D universe" in which possible answers to some of the most profound questions of physics are hidden.

In the face of these vast unknown sectors of the universe any observational probe into its past history is invaluable. Recently, the direct measurement of the expansion rate, expressed in terms of the Hubble parameter $H(z)$, is gaining increasing attention. As a cosmological test, it can help with the determination of important parameters that affects the evolution of the universe, and reconstruct the history around key events such as the turning point from deceleration to acceleration. As observable, it manifests itself in various forms in different eras, especially in the baryon acoustic oscillation (BAO) features in the LSS that may be detectable in the dark age.

This paper is a review on the current status of observational Hubble parameter data and its application in cosmology. In Section 2, we briefly review the cosmological background of an expanding universe. In Section 3, we present two important observational methods of $H(z)$ observation, their principles, and implementations. Next, we review the important role of the observational $H(z)$ data in the study of cosmological models in Section 4. We will also discuss some issues associated with their application. Finally, in Section 5, we briefly discuss some ongoing efforts that promise possible improvements over the current status of $H(z)$ measurements.

2. Background

In this section, we will review some basic ideas and definitions in cosmology that must be kept in mind in order to understand and interpret the observational $H(z)$ data and their implications.

2.1. Spacetime, Metric, and Coordinates. The spacetime structure of the homogeneous, isotropic, and spatially flat universe is characterized by the Friedmann-Robertson-Walker (FRW) metric

$$g_{\mu\nu} = \begin{pmatrix} -1 & & & \\ & a^2(t) & & \\ & & a^2(t) & \\ & & & a^2(t) \end{pmatrix}. \tag{2}$$

The presence of the scale factor $a(t)$ means that the spacetime is not necessarily static. In reality, we know that the universe is expanding and $a(t)$ increases with time.

Using the metric (2), the infinitesimal spacetime interval scalar $\mathrm{d}s^2 = \mathrm{d}x_\nu \mathrm{d}x^\nu = g_{\mu\nu}\mathrm{d}x^\mu \mathrm{d}x^\nu$ is obviously

$$\mathrm{d}s^2 = -c^2\mathrm{d}t^2 + a^2(t)\mathrm{d}x^i\mathrm{d}x^i. \tag{3}$$

Here, we have used the four-coordinate vector $x^\alpha = (ct, \mathbf{x}^i)$ that has the dimension of length.

It is often useful to express the spatial components of the four-coordinate vector, that is, the "comoving position," in dimensionless spherical coordinates $\mathbf{x}^i = (r, \theta, \phi)$ in order to extend the metric to nonflat situations, and give the scale factor the dimension of length. Under this convention, the spacetime interval (3) can be rewritten as

$$\mathrm{d}s^2 = -c^2\mathrm{d}t^2 + a^2(t)\left(\frac{\mathrm{d}r^2}{1-kr^2} + r^2\mathrm{d}\theta^2 + r^2\sin^2\theta\mathrm{d}\phi^2\right), \tag{4}$$

where k is one of $\{-1, 0, 1\}$. The parameter k is the sign of the spatial curvature, and $k = 0$ if the universe is spatially flat.

We can further transform (4) by introducing the coordinate

$$\chi = \int_0^r \frac{\mathrm{d}r'}{\sqrt{1-kr'^2}} = \mathrm{sinn}^{-1} r, \tag{5}$$

where the sinn function is a shorthand notation

$$\mathrm{sinn}x = \begin{cases} \sin x & \text{for } k = 1, \\ x & \text{for } k = 0, \\ \sinh x & \text{for } k = -1. \end{cases} \tag{6}$$

Switching to the spatial coordinates (χ, θ, ϕ), the interval $\mathrm{d}s^2$ can be written as

$$\mathrm{d}s^2 = -c^2\mathrm{d}t^2 + a^2(t)\left[\mathrm{d}\chi^2 + \mathrm{sinn}^2\chi\left(\mathrm{d}\theta^2 + \sin^2\theta\mathrm{d}\phi^2\right)\right]. \tag{7}$$

The physical interpretation of χ can bee seen by placing ourselves at the origin $r = 0$ and considering a distant, comoving photon emitter in our line-of-sight direction with the coordinate $r = r_e$. Rotating the coordinates so that the direction of the emitter has $\theta = 0, \phi = 0$, we find

$$\mathrm{d}s^2 = -c^2\mathrm{d}t^2 + a^2(t)\frac{\mathrm{d}r^2}{1-kr^2} \tag{8}$$

along the line-of-sight. Let t_e be the time of photon emission and t_0 that of its reception. Since light-like worldlines have $\mathrm{d}s^2 = 0$, we find, for the photon

$$\int_{t_e}^{t_0} \frac{c\mathrm{d}t}{a(t)} = \int_0^{r_e} \frac{\mathrm{d}r}{\sqrt{1-kr^2}} = \chi(r_e). \tag{9}$$

Consider the integrand in the left-hand side of (9). The line element $\mathrm{d}x = c\mathrm{d}t$ is the physical distance and the photon has traveled during the time interval $\mathrm{d}t$. But by dividing the physical distance by $a(t)$, we get the comoving distance, therefore, χ can be interpreted as the total, integrated comoving distance between the emitter and us. If the space is flat, this comoving distance is just the difference in the radial coordinate $\Delta r = r_e - 0 = r_e$.

Sometimes it is convenient to introduce the *conformal time*, or the *comoving horizon* η as the time component of the four-coordinate. The conformal time is defined as

$$\eta(t) = \int_0^t \frac{\mathrm{d}t'}{a(t')}, \tag{10}$$

where we integrate from the "beginning of time." Using $c\eta$ as the time component, the comoving four-coordinate can be

written as a dimensionless vector $x^\alpha = (c\eta, \chi, \theta, \phi)$ and the FRW metric takes the form

$$g_{\mu\nu} = a^2(\eta)\begin{pmatrix} -1 & & & \\ & 1 & & \\ & & \sinn^2\chi & \\ & & & \sinn^2\chi\sin^2\theta \end{pmatrix}. \quad (11)$$

2.2. Expansion, Redshift, and the Hubble Parameter. In the introduction, we mentioned Hubble's Law discovered in 1929. Hubble's original paper had profound impact upon the history of astrophysics and, to a greater extent, mankind's perception of the universe, but here we only take some time to appreciate two of his timeless insights.

At the end of his paper, Hubble briefly discussed the possible mechanisms for "displacements of the spectra" (i.e., redshift, in modern terms) in the de Sitter cosmology model in which the expansion of the universe is dominated by a vacuum energy. He pointed out the two sources of the redshift: the first being "an apparent slowing down of atomic vibrations" and the other attributed to "a general tendency of material particles to scatter." In today's words, the first is the special-relativistic effect of Doppler shift caused by the peculiar motion of galaxies and the latter the general-relativistic, *cosmological redshift* which is linked to the expansion of the comoving grid itself. In the rest of this article, we will see how these two effects arise in modern cosmology and end up in our observational figures.

Hubble also noted that his proportional law might be "a first approximation representing a restricted range in distance," therefore deviating from the pure de Sitter model in which the Hubble constant H should indeed be constant everywhere and throughout the history. This is exactly how we see it now. In the contemporary context, we usually define the *Hubble parameter* H to be the relative expansion rate of the universe

$$H = \frac{\dot{a}}{a}, \quad (12)$$

and its value is usually expressed in the unit of $\mathrm{kms}^{-1}\mathrm{Mpc}^{-1}$. The Hubble *constant*, H_0, now officially refers to the current value of the Hubble parameter.

However, it is not apparent how this definition is related to observable quantities. Therefore, we have to relate (12) to physical observables such as the length, the time, and the redshift.

First, we note that the cosmological redshift z at any time t is related to the scale factor a. Let t_e be the time of a photon's emission by a distant source and t_0 the time of its reception by an observer "here and now." The observed redshift z of the source satisfies

$$1 + z = \frac{a(t_0)}{a(t_e)}. \quad (13)$$

Consider an observer who surveys various sources with different redshifts. The ideal survey is assumed to complete instantly: all the observations are done at exactly the same time instance t_0. Of course, this is not strictly true, but we do not expect the scale factor $a(t_0)$ to change "too fast," and we expect the redshift not to change too much during the temporal scale of our interest (i.e., typical lifetime of humans or observation programs). If we do allow t_0 to change, however, we are led to the Sandage-Loeb test [4, 5] that observes the drifting of redshift during a long period of time. Recently, the variation in the apparent magnitude of stable sources over t_0 has also been proposed as a possible cosmological test [6]. To our best knowledge, no data have been produced using these methods by now, and the proposed observation plans usually require $\sim$10 years to yield meaningful results [7, 8] (however, we note that the idea of "real-time cosmology" is gaining interest recently, as reviewed by Quercellini et al. [9]). In this paper we will not focus on these methods and we therefore neglect the passing of t_0.

We, therefore, differentiate (13) with respect to t_e, setting t_0 as a constant

$$\frac{\mathrm{d}a(t_e)}{\mathrm{d}t_e} = -\frac{a(t_0)}{(1+z)^2}\frac{\mathrm{d}z}{\mathrm{d}t_e} = -\frac{a(t_e)}{1+z}\frac{\mathrm{d}z}{\mathrm{d}t_e}. \quad (14)$$

Dividing both sides by $a(t_e)$, we immediately find

$$H(z) = -\frac{1}{1+z}\frac{\mathrm{d}z}{\mathrm{d}t_e}. \quad (15)$$

In Section 3.1, we will see how (15) is useful in measuring $H(z)$ by observing passively evolving galaxies.

Another way to relate $H(z)$ to observable quantities is to use the notion of the comoving distance χ introduced in (5). Take the time derivative of (9), we find

$$\frac{\mathrm{d}\chi}{\mathrm{d}t_e} = -\frac{c}{a(t_e)}. \quad (16)$$

On the other hand, (14) tells us about another derivative $\mathrm{d}t_e/\mathrm{d}z$. Therefore, we can find the derivative of χ with respect to the redshift

$$\begin{aligned}\frac{\mathrm{d}\chi}{\mathrm{d}z} &= \frac{\mathrm{d}\chi}{\mathrm{d}t_e}\frac{\mathrm{d}t_e}{\mathrm{d}z} = \frac{c}{a(t_e)}\frac{a(t_e)}{(1+z)}\frac{\mathrm{d}t_e}{\mathrm{d}a(t_e)} \\ &= \frac{ca(t_e)}{a(t_0)}\frac{\mathrm{d}t_e}{\mathrm{d}a(t_e)} = \frac{c}{a(t_0)H},\end{aligned} \quad (17)$$

that is,

$$\frac{\mathrm{d}\left[a(t_0)\chi\right]}{\mathrm{d}z} = \frac{c}{H(z)}, \quad (18)$$

(also see, e.g., [10, 11] but beware of different notation conventions). If an observable object spans the length $a(t_0)\Delta\chi$ along the line-of-sight in some redshift slice Δz, we can estimate $H(z)$. But how do we find such objects, that is "standard rods"? The idea is not to use the length of a concrete object. Instead, we explore the spatial distribution of matter in the universe and focus on its *statistical* features, such as the BAO peaks in the two-point correlation function of the density field. This is another method for extracting

$H(z)$ data from observations. (The quantity $a(t_0)\chi$ can be seen as a distance measure. It is closely related to the "structure distance" $d_S = a(t_0)r$ defined by Weinberg [12, Chapter 8] that naturally arises in calculating the power spectrum of LSS. From (5), we can see that the structure distance is equivalent to $a(t_0)\chi$ if the space is flat, or if the object is not too far away.)

We remark that the derivation of $H(z)$ expressed in terms of the standard rod, (18), is only part of the story, for we have only considered a standard rod placed in the line-of-sight direction. The transversely aligned test body is related to another important cosmological measure, namely, the angular diameter distance $D_A(z) = a(z)r(z)$. In an expanding universe, the angle $\Delta\theta$ subtended by a distant source is

$$\Delta\theta = \frac{a(z)}{D_A(z)}\Delta r_\perp = \frac{a(t_0)}{(1+z)D_A(z)}\Delta r_\perp, \tag{19}$$

where $\Delta r_\perp$ is the transverse spatial span of the source measured in the difference of comoving coordinate r [13, 14]. Naturally, once the physical scale of BAO is known and the BAO signal measured, the corresponding angular diameter distance can also be used as a cosmological test.

A classical cosmological test is the Alcock-Paczyński (AP) test [15] that can be expressed as another combination of $H(z)$ and $D_A(z)$. The observable of the AP test is the quantity $A(z) = \Delta z/(z\Delta\theta)$ of some extended, spherically symmetric sources, where Δz is the difference in redshft between the near and far ends of the object, and $\Delta\theta$ the angular diameter. By our (18) and (19), it can be expressed as

$$A(z) = \frac{\Delta z}{z\Delta\theta} = \frac{1+z}{z}D_A(z)H(z)\frac{\Delta\chi}{\Delta r_\perp}. \tag{20}$$

A well-localized object placed in a region not too far away from us (so the nontrivial spatial geometry can be neglected) will have $\Delta\chi \approx \Delta r_\parallel$, the difference in the comoving coordinate along the line-of-sight. Furthermore, for a nearly spherical object the approximation $\Delta r_\parallel \approx \Delta r_\perp$ holds and $A(z)$ is reduced to

$$A(z) = \frac{1+z}{z}D_A(z)H(z). \tag{21}$$

Clearly, it cannot constrain $H(z)$ or $D_A(z)$ separately, but a combination of both. The AP test, in more modern context, is usually understood as a geometrical effect on the statistical distribution of objects instead of concrete celestial bodies (see [16–18], and also [10, 19] where the BAO effects were explicitly treated in the analysis).

Another combination of $H(z)$ and $D_A(z)$ naturally arises in the application of BAO scales measured in the spherically averaged galaxy distribution, namely, the distance measure D_V [20] defined by

$$D_V(z) = \left[\frac{cz(1+z)^2D_A^2(z)}{H(z)}\right]^{1/3}. \tag{22}$$

To break the degeneracy between $H(z)$ and $D_A(z)$ in $D_V(z)$, the full 2-dimensional galaxy distribution must be used, with the correlation function conveniently decomposed into the line-of-sight and transverse components (see Section 3.2, but also see [21] for another decomposition scheme).

3. Hubble Parameter from Observations

Equations (15) and (18) are the bare-bone descriptions of two established methods for $H(z)$ determination: the differential age method and the radial BAO size method, respectively. Either has been made possibly only by virtue of state-of-the-art redshift surveys such as the Sloan Digital Sky Survey (SDSS) [22]. In this section, we will review both methods and the data they produced.

3.1. The Differential Age Method. As (15) suggests, to apply age-dating to the expansion history, we look for the variation of ages, Δt, in a redshift bin Δz [23]. The aging of stars serves as an observable indicator of the aging of the universe, because the evolution of stars is a well-studied subject, and stars' spectra can be taken and analysed to reveal information about their ages. However, at cosmological distance scales, it is not practical to observe the stars one by one: we can only take the spectra of galaxies that are ensembles of stars, possibly of different populations. Since different star populations are formed at drastically different epochs, it is important for us to identify galaxies that comprises relatively uniform star populations, and to look for more realistic models of star formation.

The identification of such "clock" galaxies and the observation of their spectra have been carried out for archival data [24], and surveys such as the Gemini Deep Deep Survey (GDDS) [25], VIMOS-VLT Deep Survey (VVDS), and the SDSS [26]. In addition, high-quality spectroscopic data have been acquired from the Keck I telescope for red galaxies in galaxy clusters [27]. Among the galaxies being observed, special notices should be paid to the luminous red galaxies (LRGs). LRGs are massive galaxies whose constituent star populations are fairly homogeneous. They make up a fair proportion in the SDSS sample and, beyond serving as "clocks," also trace the underlying distribution of matter in the universe (albeit with bias). Therefore, they reveal BAO signature in the density autocorrelation function that is used as the "standard rod" in the size method.

The identification and spectroscopic observations of these galaxies have led to direct determinations of $H(z)$ in low and intermediate redshift ranges. Jimenez et al. [24] first obtained a determination of $H(z) = 69 \pm 12\,\mathrm{km\,s^{-1}\,Mpc^{-1}}$ at an effective redshift $z \approx 0.09$ by the differential age method. The work was later expanded by Simon et al. [28] who extended the determination of $H(z)$ to 8 more redshift bins up to $z \approx 1.8$. This dataset was brought up-to-date by Stern et al. [26, Table 2]. Recently, new age-redshift datasets for different galaxy velocity dispersion groups have been made available [29] from SDSS data release (DR) 7 LRG samples. We will see how these data are used in the study of cosmology models in Section 4.

One may wonder why we take the effort to calculate the age differences in redshift bins when the age (or lookback time) data themselves can also be used to test

cosmological models. Indeed, the absolute age has been very useful in the estimation of cosmological parameters [30–33]. Nevertheless, precise age-dating with low systematic biases can be only carried out on a narrow selection of sources. On the other hand, by taking the difference of the ages in narrow redshift bins, the systematic bias in the absolute ages can hopefully cancel each other [34]. Of course, we are not gaining anything for nothing even if the systematics perfectly cancel, for the binning of data lowers the total amount of measurements we can have.

A further approximation is that the majority of stars in the galaxies are formed almost instantaneously, in a single "burst" [35]; therefore the intrinsic spread of the measured age arising from a heterogeneous star formation history can be expected to be small when fitting the observed spectra to stellar population models (specifically the single-stellar population (SSP) model used in [28] and [26]). However, recent developments in the study of the formation history of galaxies and their stellar populations have led us to reconsider the assumptions made in previous works. For example, using galaxy samples selected from numerical simulations, Crawford et al. [36] have shown that the SSP assumption may contribute to the systematic bias that varies across redshift ranges (hence failing to cancel, and propagating into the differential ages), while models that take the extended star formation history into account can be used to reduce the errors on $H(z)$.

In addition to the complexities in the stellar populations in each galaxy, the heterogeneity of galaxies in the sample also contributes to the errors in $H(z)$ measurements. In [36], new sample selection criteria have been proposed that could help with obtaining more homogeneous galaxy samples for future analyses.

3.2. The Radial BAO Size Method. In Section 2.2, we mentioned that the "standard rod" we seek in the sky is not an actual object but a statistical feature. Indeed, the physical sizes of distant celestial objects are usually poorly known. Worse still, even the *apparent*, that is angular, sizes of galaxies are ambiguous because galaxies do not show sharp edges and they appear fuzzy in images. It can be imagined that size measurements along the line-of-sight could only lead to more problems, because even the angular sizes cannot help us much in this case. Therefore, identifying a statistical "standard rod" becomes a necessity.

In the study of LSS, correlation functions are a simple and convenient measure of the statistical features in the spatial distribution of matter in the universe. (For an early yet important treatment of the topic in the context of galaxy surveys, see [37]. For an example of other statistics in the context of BAO, see [38].) The two-point autocorrelation (i.e., the correlation of a density field with itself) function $\xi(\mathbf{r}_1, \mathbf{r}_2)$ is one of the most used member in the correlation function family. It measures the relatedness of position pairs in the same density field: the joint probability of finding two galaxies in volume elements $\mathrm{d}V_1$ and $\mathrm{d}V_2$ located in the neighborhood of spatial positions $\mathbf{r}_1$ and $\mathbf{r}_2$, respectively, is

$$\mathrm{d}P_{12} = n^2[1 + \xi(\mathbf{r}_1, \mathbf{r}_2)]\mathrm{d}V_1\mathrm{d}V_2, \tag{23}$$

where n is the mean number density. If we believe that our universe is homogeneous in a statistical sense (i.e., that the probabilistic distribution, or ensemble, from which the densities anywhere in our particular instance of the universe is drawn, does not vary from one area of the universe to another), the autocorrelation function becomes a function of $\mathbf{r} = \mathbf{r}_1 - \mathbf{r}_2$ only. If we further assumes the (statistical) isotropy of the universe, the direction of $\mathbf{r}$ becomes unimportant, and the autocorrelation is dependent on the magnitude of $\mathbf{r}$ only (i.e, $\xi = \xi(r)$). Actually, our assumption of homogeneity is unnecessarily strong if we only work with two-point statistics and all we need is the homogeneity in the first two moments of the underlying ensemble. Such an ensemble is known as a wide-sense stationary (WSS) one.

For a WSS ensemble, the famous Wiener-Khinchin theorem says that the autocorrelation and the power spectrum $P(\mathbf{k})$ form a Fourier transform pair

$$\begin{aligned} P(k) = P(\mathbf{k}) &= \int \xi(\mathbf{r}) e^{i\mathbf{k}\cdot\mathbf{r}} \mathrm{d}^3 r, \\ \xi(r) = \xi(\mathbf{r}) &= \frac{1}{(2\pi)^3} \int P(\mathbf{k}) e^{-i\mathbf{k}\cdot\mathbf{r}} \mathrm{d}^3 k. \end{aligned} \tag{24}$$

(Here we write the power spectrum as $P(\mathrm{k})$, independent of the direction of the wave vector $\mathbf{k}$, under the same assumption of statistical isotropy mentioned above, but see discussion about redshift distortion below.) Therefore, either the power spectrum or the autocorrelation can serve as a statistical tool to reveal the information contained in the LSS. Methods of estimating $P(k)$ have been developed and the importance of the power spectrum emphasized [39, 40]. On the other hand, for BAO surveys, the autocorrelation function is probably a more straightforward way of presenting the results and testing their significance, because the BAO scales manifest themselves as protruding features ("peaks" or "bulges") in $\xi(r)$. Actually, an estimator to the autocorrelation, along with its variance, can also be conveniently constructed from survey data using pair counts between the survey and random fields [41].

Needless to say, the "true" autocorrelation of the ensemble can never be fully known, because we have only one realization of the random field which is *the* universe we live in. However, *estimating* the autocorrelation still makes sense because for today's large and well-sampled surveys, the assumption of ergodicity is valid, under which the statistics can be performed to infer knowledges about the underlying ensemble [12, Chapter 8 and Appendix D].

Thus, if a random process induces some features in the spatial distribution of matter, the autocorrelation can be numerically computed to reveal such features that are otherwise hidden in the seemingly stochastic distribution. Furthermore, if the mechanism and properties of this process are well understood and quantitatively modelled, parameter estimation using these features becomes a possibility.

One of such possibility is provided by the BAO signatures in the LSS. The mechanism of BAO effects must be traced back to the early universe before recombination, when the Compton scattering rate was much higher than the cosmic

expansion rate. Under this extreme limit, the tightly coupled photons and baryons can be treated as a fluid in which the perturbations drive sound waves. The BAO effect in the cosmic microwave background (CMB) radiation has been subjected to extensive theoretical studies (see the early work of Peebles and Yu [42], a powerful analytical treatment by Hu and Sugiyama [43] in Fourier space, another by Bashinsky and Bertschinger [44] in position space, and a review by Hu and Dodelson [45]). It has been confirmed and measured by CMB observations such as the Wilkinson Microwave Anisotropy Probe (WMAP) [46–50]. We will not discuss CMB in detail, and mainly concern ourselves with the aftereffect of BAO, namely, its imprints on the large-scale distribution of matter.

The imprints of BAO in the observable distribution of galaxies today was predicted in theory (see [51, 52], and note that these papers were mainly written in the language of $P(k)$ rather than $\xi(r)$). They were first detected in SDSS data by Eisenstein et al. [53]. In [20], BAO measurements were made for SDSS and 2dF survey data using the power spectrum and the results were presented as a general test of cosmological models. The usage of BAO signatures in the LSS as a probe of $H(z)$ was discussed in [10] (see also [54–56]).

The idea of using BAO scales may appear to be simple and straightforward by our description so far, but in reality the autocorrelation function is subjected to various distortion effects that must be accounted for.

First, galaxies are not comoving objects. Their apparent redshifts are inevitably a combined effect of the cosmological redshift and peculiar velocities (which was once contemplated by Hubble, see Section 2.2). Peculiar motion distorts the apparent correlation pattern in the redshift space and makes it anisotropic (see [57, 58]). Therefore, the isotropic autocorrelation function $\xi(r)$ fails to be a good measure. In the literature, the autocorrelation is usually expressed as a function of scales in the radial (line-of-sight) direction π and transverse direction σ: $\xi = \xi(\sigma, \pi)$ with $r = \sqrt{\sigma^2 + \pi^2}$. The observed $\xi(\sigma, \pi)$ will be a convolution between $\xi(r)$ and the peculiar velocity field.

Second, geometry of the spacetime also distorts the correlation pattern as the observation goes into deeper distances, where the spacetime geometry becomes nontrivial [59]. This is not a major concern for the analyses we will review in the rest of this section, because the survey data were from our local section of the universe ($z \approx 0$), and for $H(z)$ measurements only some thin slices in the redshift space were used. However, future work that deals with deep survey data must take the geometrical distortions into analysis.

There is also the more delicate issue of biasing, meaning that the correlation pattern of the observed "indicators" does not necessarily reflect that of the underlying matter distribution [60]. Among the effects contributing to the bias, the magnification effect by weak lensing is worthy of notice for our discussion, because it has a large effect on the radial autocorrelation function [61, 62].

Using SDSS LRG samples in the redshift range $0.16 \leq z \leq 0.47$, BAO signature was detected in $\xi(\sigma, \pi)$ by Okumura et al. [63]. In their work, the magnification bias by weak lensing was neglected, but in the redshift range, it contributes little to

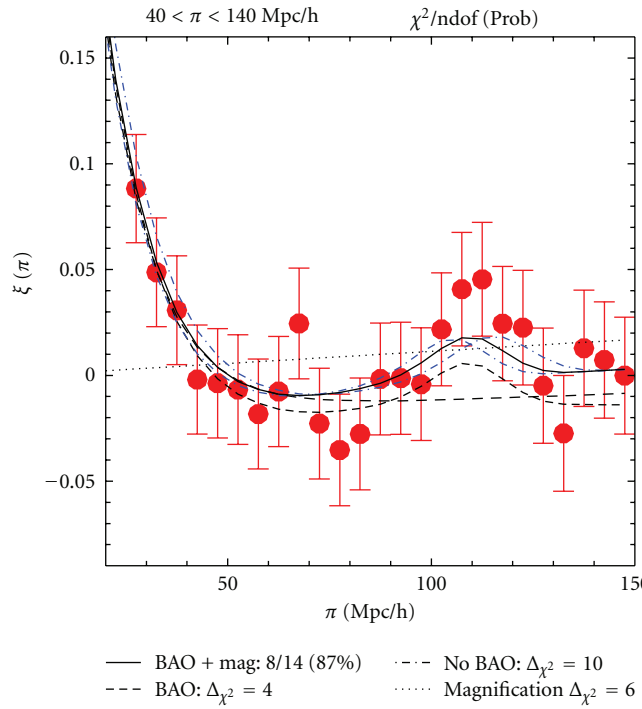

Figure 1: Detection of radial (π-direction) BAO by [64, Figure 13] in the full LRG sample. This is the correlation pattern along the π-direction and should not be confused with the monopole pattern in Figure 3 of [63]. The effect of weak lensing magnification can bee seen by comparing the solid and short dashed curves, which shows that the magnification systematically moves the peak location towards the higher scales. The dash-dotted (blue) curve shows the 1σ range by allowing the fiducial distance-redshift relation used in the analysis to vary in a parameterized way, accounting for the systematic error introduced by the mere using of a fiducial model.

the spherically averaged autocorrelation ξ_0 [61], also known as the monopole:

$$\xi_0(r) = \frac{1}{2}\int_{-1}^{1} \xi(\sigma, \pi) \mathrm{d}\mu, \tag{25}$$

where $r = \sqrt{\sigma^2 + \pi^2}$ and $\mu = \pi/r$. In [63], the BAO peak was detected in the monopole significantly, while the ridge-like BAO feature was weak in the anisotropic $\xi(\sigma, \pi)$.

Using improved LRG samples from SDSS DRs 6 and 7, and by modelling the weak lensing magnification bias, radial BAO detection and $H(z)$ measurements were made in redshift slices $z = 0.15 \sim 0.30$ and $z = 0.40 \sim 0.47$ by Gaztañaga et al. [64] (see Figure 1 for a presentation of the BAO detection). Because these redshift slices were well separated, the two measurements were independent from each other. (In previous works such as [20], the samples overlapped and the results at different z's were correlated.)

These $H(z)$ measurements were the first implementation of the radial BAO method. Due to the distortion effects, confirming the significance of the baryon ridge detection becomes a demanding process, since each distortion effect has to be carefully modelled. However, exact modelling of all the distortion effects on all scales is difficult, and when such

modelling cannot be done exactly, these effects introduces systematic errors in the measurement of the BAO ridge's scale.

Despite these, the radial BAO size method still surpasses the age method in precision. In fact, the combined statistical and systematic uncertainties presented an precision of ∼4% in $H(z)$ [64, Table 3]. This is intuitively perceptible. As we have seen in Section 3.1, the age method is affected by the (possibly very large) systematic errors in age determination. Since we can measure spatial quantities of galaxies, that is the distribution of their positions, with much greater accuracy than we can do with temporal quantities related to some vaguely defined event (i.e., the time duration from star formation in the red galaxies to now), one may intuitively expect lower uncertainties from the radial size method than the differential age method.

A subtle issue of possible circular logic in the analysis also contributes to the systematic errors in this method. In [64], a fiducial flat ΛCDM model and parameters were used to convert redshifts into distances and to gauge the comoving BAO scales in the selected redshift slice, r_{BAO} to that of the CMB measured by 5-year WMAP, $r_{\mathrm{WMAP}} = 153.3 \pm 2.0\,\mathrm{Mpc}$ (see [65]) to yield the estimation $H_{\mathrm{BAO}}(z)$

$$\frac{H_{\mathrm{BAO}}(z)}{r_{\mathrm{BAO}}} = \frac{H_{\mathrm{fid}}(z)}{r_{\mathrm{WMAP}}}, \tag{26}$$

where

$$H_{\mathrm{fid}}(z) = H_0\sqrt{\Omega_{\mathrm{m}}(1+z)^3 + (1-\Omega_{\mathrm{m}})} \tag{27}$$

and $\Omega_{\mathrm{m}} = 0.25$. (Another way to present the measurement results for use in cosmological parameter constraint $\Delta z_{\mathrm{BAO}} = r_{\mathrm{BAO}}H(z)/c$. Schematically, this is done by approximating the derivative in (18) with a ratio of differences, and identifying the interval $a(t_0)\Delta\chi$ with the measured comoving BAO scale. In Section 4, we briefly discuss its usage.) The use of a fiducial model introduces bias in all measurements, which is hard to model exactly, but an analysis of this effect was performed using Monte Carlo simulations so that its contribution to the systematic uncertainties could be assessed. The authors of [64] hence argued that the measurement results are model independent, therefore useful as a general cosmological test. The reader may also consult [20] for a different approach to this issue, using cubit spline fit of the distance-redshift relation so that the result could be applied to a large class of models without having to reanalyze the power spectra for each model to be tested.

3.2.1. A Word on the Dispute over the Radial BAO Detection. Currently, there is some dispute over the claimed detection of radial BAO and measurement of $H(z)$ in [64]. Miralda-Escudé [66] argued against the methods in [64] and the statistical significance of the claimed BAO detection. Kazin et al. [67] analyzed the SDSS DR7 sample of LRGs and obtained similar results to [64], but offered another interpretation using the χ^2/(degree of freedom) statistic and the Bayesian evidence [68] that disfavors a statistically significant detection. On the other hand, the recent research of Tian et al. [69] claims that the radial BAO feature is not a fluke, albeit certain assumptions made this reassessment somewhat optimistic. The authors of [64] also defended their work in [70]. We refer to these variety of arguments and opinions to remind the reader of these ongoing investigations. Nevertheless, we believe that the general method of measuring $H(z)$ using radial BAO is well-motivated and promising regardless of its current implementation, as it is expected to give more definitive results of radial BAO and $H(z)$ measurement with upcoming redshift survey projects [67].

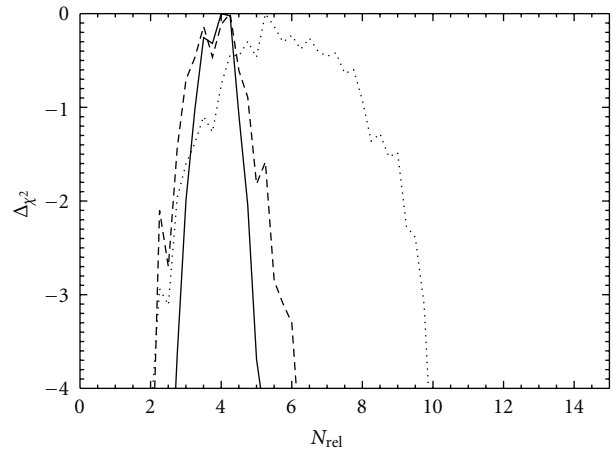

Figure 2: Constraint on the effective number of relativistic neutrino species, N_{rel}, by Stern et al. [26] using their $H(z)$ measurements by the differential age method. Dotted line plots the 5-year WMAP [71] likelihood, dashed line plots the likelihood with WMAP and H_0 determined by Riess et al. [72], and the solid like the likelihood with WMAP, H_0 and $H(z)$ data. Adding $H(z)$ data helped refining the constraint to $N_{\mathrm{rel}} = 4 \pm 0.5$ at 1-σ level. The improvement in the constraint by adding $H(z)$ data is evident. Note that this figure displays the deviation of the χ^2 statistic from its minimum *inverted* ($\Delta\chi^2 = \chi^2_{\mathrm{min}} - \chi^2$). The intersections of the $\Delta\chi^2$ plots with the constant $\Delta\chi^2 = 4$ line correspond to 2-σ constraints.

4. Observational Hubble Parameter As a Cosmological Test

The efforts in obtaining observational $H(z)$ data was certainly done with the goal of testing cosmological models in mind. In [24], the observation $H(z)$ at $z \approx 0.09$ was used to constrain the equation of state parameter of dark energy. In [28], the redshift-variability of a slow-roll scalar field dark energy potential was constrained by the differential age $H(z)$ data. The same dataset was also utilized in the study of the ΛCDM universe, especially the summed neutrino masses m_ν, the effective number of relativistic neutrino species N_{rel}, the spatial curvature Ω_k, and the dark energy equation of state parameter ω [73]. The updated $H(z)$ data presented in [26] was used by their authors to improve the results obtained in earlier papers.

In particular, the combination of CMB and $H(z)$ observation is a very effective way to constrain N_{rel} ([74], see the reproduced Figure 2 in this paper). In this paper, we will

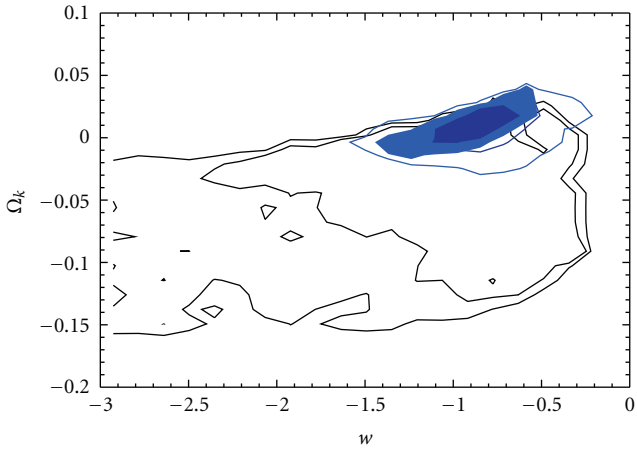

FIGURE 3: Joint constraint on the energy density corresponding to the spatial curvature, Ω_k, and the dark energy equation of state parameter, w, by Stern et al. [26]. The large, irregular regions bounded by dark contours were from 5-year WMAP alone. The blue contours were obtained by adding H_0 constraints. Filled regions were obtained by further adding $H(z)$ data. The application of $H(z)$ data helps with breaking the degeneracy between Ω_k and w.

not go further into the topic of cosmic neutrinos, which is intrinsically related to fundamental physics. However, we should point out a remarkable result, that the $H(z)$ data, when used jointly with CMB and other late-era cosmological tests, offer valuable insight into the neutrino properties related to the much earlier universe, independent of Big-Bang nucleosynthesis (BBN) [75, 76] tests. Moreover, the BBN constraints are obtained using Helium abundance measurements that are subjected to the systematic biasing effects arising from late-time nucleosynthesis. Therefore, $H(z)$ data is an important consistency check measure in the presence of this systematic uncertainty [74].

Figure 3 shows that adding $H(z)$ data helps with breaking the degeneracy between spatial curvature and dark energy equation of state. In the ΛCDM universe, both the dark energy and spatial curvature become dominant in recent epochs. Therefore, separating their respective effects on the expansion of the universe becomes important, as well as challenging [77, 78]. While other tests using the combination of weak lensing and BAO are likely to measure the curvature distinctively in the future [11, 79], our current knowledge of $H(z)$ is still a valuable complement to other tests in the sense of DE-curvature degeneracy breaking [73].

The data produced by the BAO size method in [64] is scarcer in quantity but of higher precision. In [64], they were extrapolated to $z = 0$ to offer an independent estimation of the Hubble constant H_0 and were used to test the accelerated expansion of the universe. It has been demonstrated that the radial Δz_{BAO} measurements is able to put stringent constraints over the dark energy parameters [80].

In the papers cited above, the parameter constraints obtained from observational $H(z)$ data were shown to be consistent with other cosmological tests, such as the CMB anisotropy. In this way, the observational $H(z)$ data presents

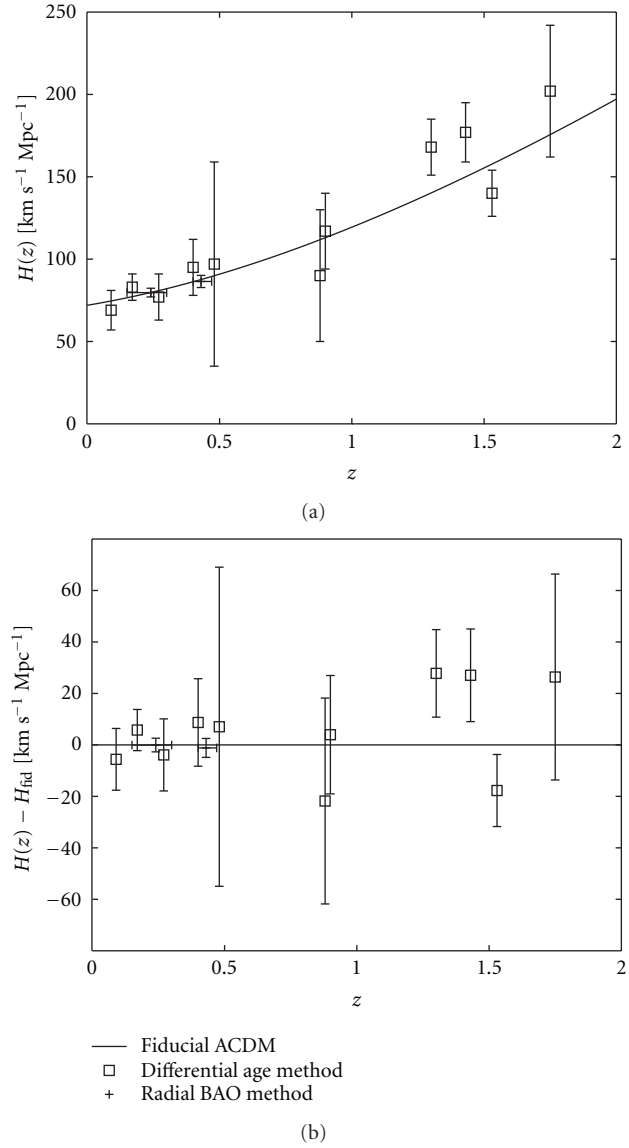

FIGURE 4: (a) the available $H(z)$ data from both differential age method and radial BAO size method (see Table 1 and references therein). The solid curve plots the theoretical Hubble parameter H_{fid} as a function of z from the spatially flat ΛCDM model with $\Omega_{\mathrm{m}} = 0.25, \Omega_\Lambda = 0.75$, and $H_0 = 72\,\mathrm{km\,s^{-1}\,Mpc^{-1}}$. (b) the same data, but the residuals with respect to the theoretical model H_{fid} are plotted. In both panels, the z error bars on the measurements from the radial BAO method are used to mark the extents of the two independent redshift slices in which the BAO peaks were measured.

themselves as a useful, *independent* cosmological test. In particular, it serves as a powerful tool to break the degeneracy between the curvature and dark energy parameters.

These up-to-date data are summarized in Table 1. In Figure 4 we plot the $H(z)$ data versus the redshift. To help visualizing the data, we also plot a spatially flat ΛCDM model with $\Omega_{\mathrm{m}} = 0.25, \Omega_\Lambda = 0.75$, and $H_0 = 72\,\mathrm{km\,s^{-1}\,Mpc^{-1}}$.

In addition to the above authors, the observational $H(z)$ datasets have been widely used to put various cosmological

Table 1: The set of available observational $H(z)$ data.

z	$H(z) \pm 1\sigma$ error[a]	References	Remarks
0.09	69 ± 12	[24, 26]	
0.17	83 ± 8	[26]	
0.24	79.69 ± 2.65[b]	[64]	In the redshift slice $0.15 \sim 0.30$
0.27	77 ± 14	[26]	
0.4	95 ± 17	[26]	
0.43	86.45 ± 3.68[b]	[64]	In the redshift slice $0.40 \sim 0.47$
0.48	97 ± 62	[26]	
0.88	90 ± 40	[26]	
0.9	117 ± 23	[26]	
1.3	168 ± 17	[26]	
1.43	177 ± 18	[26]	
1.53	140 ± 14	[26]	
1.75	202 ± 40	[26]	

[a] $H(z)$ figures are in the unit of km s^{-1} Mpc^{-1}.

[b] Including both statistical and systematic uncertainties, $\sigma = \sqrt{\sigma_{\text{sta}}^2 + \sigma_{\text{sys}}^2}$.

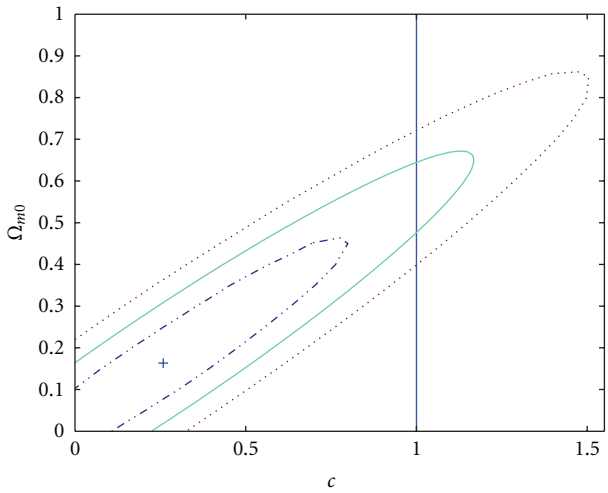

Figure 5: Parameter constraints for the holographic dark energy model in the Ω_m-c plane, by Yi and Zhang [81]. The constraints were obtained using age-determined $H(z)$ data in [28] alone. The cross in the lower-left marks the best-fit value. The dash-dotted, solid, and dotted contours mark the 68.3%, 95.4%, and 99.7% confidence regions, respectively. Although some degeneracy exists, it is evident that the data favor models with $c < 1$.

models under test. The first adopters included Yi and Zhang [81] and Samushia and Ratra [82] who made use of the $H(z)$ results of [28] in the study of dark energy. In [81], the $H(z)$ data alone were used to constrain the parameters of the holographic dark energy model, especially th c parameter that determines the dynamical history of the expanding universe (see Figure 5). The same dataset has also been used to study modified gravity theory such as $f(R)$ gravity in the context of cosmology [83]. The updated data in [26] and [64] have been adopted to constrain the parameters in more exotic dark energy models, for example [84, 85].

Beyond parameter constraints, the observational $H(z)$ data are also applicable in non-parametric, model-independent cosmological tests. For example, the Om statistic by Sahni et al. [86], defined by

$$Om(z) = \frac{h^2(z) - 1}{(1+z)^3 - 1}, \tag{28}$$

where h is the dimensionless Hubble parameter, $h = H(z)/H_0$. This statistic is useful as a null test of dark energy being a cosmological constant Λ and is more robust than parameterizations of the dark energy equation of state. Another result for testing Λ that incorporates $H(z)$ data (the $\mathcal{L}_{\text{gen}}$ test) is given by Zunckel and Clarkson [87] with the addition of distance information. In either paper however, the Hubble parameter data used were not the independent observational measurements discussed in this review, but the ones reconstructed using SNIa luminosity distances. In a similar fashion, it has been shown that $H(z)$ and distance measurements can further test the spatial flatness of the universe, or even the Copernican Principle of large-scale homogeneity and isotropy that is behind the mathematical form of the FRW metric (2) by a model-independent approach [88, 89]. In [89], the use of $H(z)$ in some of these tests was demonstrated with real-world observational data reviewed here.

Despite the wide application of the $H(z)$ datasets in the literature, we would like to point out some issues associated with their usage.

First, in some papers [84, 85, 90] that made use of $H(z)$ data derived from radial BAO by Gaztañaga et al. [64] in χ^2 analyses, the measurement at a middle redshift $z = 0.34$ was used in conjunction with those from the two independent redshift slices near $z = 0.24$ and 0.43, under the tacit assumption of being independent from each other. However, this is not true, because the determination at the middle redshift was not made from a separate, non-overlapping redshift slice, but from the whole sample of galaxies, *including* the lower and upper redshift ranges. If the

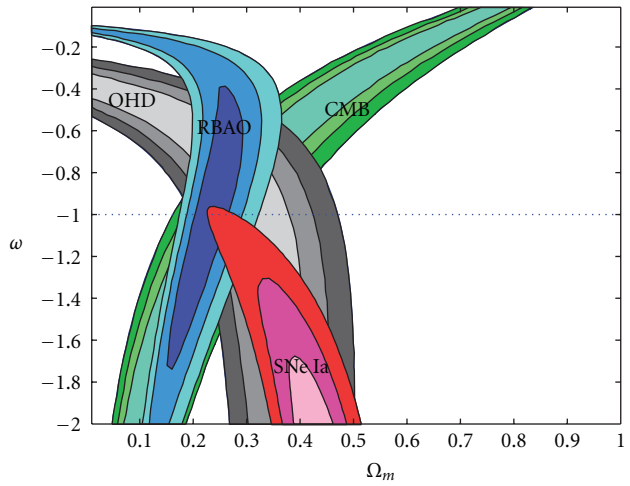

Figure 6: Possible tension between $H(z)$ and type Ia supernovae data depicted in the χ^2 fitting results for the spatially flat XCDM model (similar to ΛCDM, except that the dark energy equation of state parameter ω is set free instead of being fixed at $\omega = -1$). The SN data favor a phantom dark energy with $\omega < -1$ while other data, including observational $H(z)$ (OHD), are consistent with ΛCDM. The OHD used in this figure were the measurements by [28] using the differential age method, and the SN data were from [93]. The RBAO contours were found using the Δz_{BAO} data in [64]. Confidence regions are 68.3%, 95.4%, and 99.7%, respectively. This figure first appeared in [91, Figure 4].

data is to be used in quantitative works, this interdependency should not be ignored and must be explicitly analysed. A related issue is combining the $H(z)$ data determined from radial BAO peaks with the Δz_{BAO} data derived using the same method under the assumption of their independence (this practice can be found, e.g., in [90]). To be rigorous (or pedantic, depending on your point of view), we do not believe that this is the best way to use the data, and we insist on an analysis involving the (nondiagonal) covariance between these datasets. On the other hand, the combination of Δz_{BAO} data and *age*-dated $H(z)$ is mostly free from this interdependence problem and they actually complement each other well [91, in particular, Figures 1 and 2]. We also note that in qualitative explorations one may choose to relax this restriction to some reasonable extent, for example, in the discussion of accelerate expansion in [64, Section 4.4].

Another topic that could be worthy of future discussions is the possible tension between the $H(z)$ datasets and other observational data. As noted by Figueroa et al. [73], datasets of different physical natures and systematic effects can be safely combined only if they agree with each other well (see also [92]). In this regard, we note that there is possibly some tension between $H(z)$ and type Ia supernova (SNIa) luminosity distances as shown in [91] (see Figure 6). However, this apparent tension could be statistical in nature and may simply be a consequence of not having enough independent measurements of $H(z)$. We hope that future expanded $H(z)$ datasets would allow us to check its consistency with other data in a quantitative manner.

5. Future Directions

The available $H(z)$ data have so far proven to be a useful tool in the pursuit of understanding the expansion history of the universe and the possible nature of dark energy. However, these datasets do not have very good redshift coverage. The current measurements have gone as deep as $z = 1.75$, and this redshift range is only sparsely covered. There is also another issue of the large error bars associated with the $H(z)$ figures from the differential age method. On the other hand, the collection of more and higher quality $H(z)$ data will not only help us constrain the parameters, but will also allow us to understand the possible tension between $H(z)$ and other cosmological tests. The latter is important, because tension is usually an indicator of systematic errors in the data. By understanding the tension, we may finally conquer the systematic effects that have not yet been modelled well enough.

In this section, we will describe a few directions of future cosmological observations and their implications in the measurements of the Hubble parameter.

5.1. Future Improvements in the Differential Age Method. The relatively large uncertainties in the differential age method could be partially compensated if future datasets could offer better coverage in the redshift range accessible by this method. Using mock data, we recently estimated that future $H(z)$ datasets would offer similar or even higher parameter-constraining power compared with current SNIa datasets if it could add as many as ~60 independent measurements to cover the redshift range $0 \leq z \leq 2$ [94]. To achieve this level of data coverage, future surveys must be able to offer a large sample of LRGs to be used in age-dating. According to [28], the Atacama Cosmology Telescope (ACT) [95] can be utilized in the future to identify passively evolving, red galaxies by their Sunyaev-Zel'dovich effect. These galaxies can in turn be spectroscopically measured and age-dated, and it has been estimated that they could yield ~1000 $H(z)$ measurements. This means the quality of current differential age $H(z)$ data can be expected to increase significantly.

The error model used in the analysis of differential age $H(z)$ data in [94] was empirical, which may have underestimated possible future improvements. In [36], it has been estimated that $H(z)$ may be measured within 3% relative error at $z \approx 0.42$ in realistic observations if the star formation systematics could be properly accounted for. This level of precision is on par with the current status of the radial BAO method, and we hope it could be achieved in the near future.

5.2. Future Improvements in the Radial BAO Size Method. The radial BAO size method has already been demonstrated to provide highly accurate $H(z)$ measurements. However, this accuracy came at a cost, for spectroscopic data must be taken for the great number of galaxies under survey to find their redshifts, which is time-consuming. Fortunately, it turns out that for low redshift ranges, photometric redshift surveys can be a sufficient and promising approach [96–98] to the detection and measurements of radial BAO features

in the autocorrelation function. Photometry has several advantages over spectroscopy: it is cheaper, faster, and able to reach fainter sources.

Shortly before this review is written, the WiggleZ redshift survey [99] of emission-line galaxies produced its first data release [100]. As the data is being released, it is expected that the radial BAO signal can be put to further scrutiny [67].

The BAO method is unique in that it allows us to reconstruct the cosmic expansion through a vast range of eras. Unlike the differential age method in which the observable indicators of time are located within a limited redshift range, BAO signal detection is possible as long as the distribution of matter, regardless of its form, can be traced. Even if the current implementation of the radial BAO method is mainly confined in the redshift range of $z \approx 0$, future redshift surveys such as the planned SDSS III project [101] are designed to reach into deeper universe and measure $H(z)$ at redshifts up to $z \approx 2.5$ by observing the Lyman-α forest absorption spectra of high-redshift quasars (see [102] for a discussion of high-z measurement of radial BAO and $H(z)$ and its implication for dark energy, and [103, 104] for numerical simulation studies). Recently, in the wake of the proposed Euclid satellite project [105, 106], the enormous potential of space-based redshift surveys in the determination of $H(z)$ and other parameters has been studied in [107]. Finally, the proposed observational programs of the 21 cm background may further extend our knowledge of $H(z)$ into even deeper redshift ranges before or near the reionization era [108–110], the "dark ages" that have not been extensively explored by current observations yet.

It is also worth noting that the previous works on the analysis and measurement of $H(z)$ from the clustering of LSS have mostly concentrated on the BAO features alone. However, Shoji et al. [111] shows that accurate estimates of $H(z)$ and $D_A(z)$ could be made using the full galaxy power spectrum in the extraction of cosmological information instead of BAO features alone, provided that the nonlinear clustering effects are well controlled. We hope that the future redshift surveys observations, as well as advances in better understanding of nonlinear-regime redshift-space distortions, could lead to successful realization of their method.

6. Summary

In this paper, we reviewed the current status of observationally measured Hubble parameter data. We presented the principle ideas behind the two important and independent methods of $H(z)$ measurement, namely, the differential age method and the radial BAO size method. Both methods have been successfully implemented over the years to yield $H(z)$ data that are of varying precision and redshift coverage, and the up-to-date results have been summarized in Table 1. These data are valuable for the study of the expanding universe. They have seen wide application by cosmologists to put various cosmological models under test, and to constrain important cosmological parameters either independently or in conjunction with data of different physical natures. However, we also pointed out several issues in the usage of observational $H(z)$ data. Finally, despite some current shortcomings, we find the $H(z)$ data of great potential, as future observational programs can be expected to improve significantly the quality of $H(z)$ data that may lead us into unexplored realms of the universe.

Acknowledgments

The authors gratefully acknowledge Chris Clarkson, Eyal A. Kazin, and Varun Sahni for their helpful suggestions. They would like to thank the anonymous referee for critically reviewing the manuscript and providing insightful comments that helped them improve this paper greatly. Cong Ma thanks Zhongfu Yu for his help in preparing some of the materials in the bibliography list. This work was supported by the National Science Foundation of China (Grants no. 10473002), the Ministry of Science and Technology National Basic Science program (project 973) under grant no. 2009CB24901, and the Fundamental Research Funds for the Central Universities.

References

[1] E. P. Hubble, "A relation between distance and radial velocity among extra-galactic nebulae," *Proceedings of the National Academy of Sciences of the United States of America*, vol. 15, pp. 168–173, 1929.

[2] A. G. Riess, A. V. Filippenko, P. Challis et al., "Observational evidence from supernovae for an accelerating universe and a cosmological constant," *Astronomical Journal*, vol. 116, no. 3, pp. 1009–1038, 1998.

[3] S. Perlmutter, G. Aldering, G. Goldhaber et al., "Measurements of Ω and Λ from 42 high-redshift Supernovae," *Astrophysical Journal*, vol. 517, no. 2, pp. 565–586, 1999.

[4] A. Sandage, "The change of redshift and apparent luminosity of galaxies due to the deceleration of selected expanding universes," *The Astrophysical Journal*, vol. 136, pp. 319–333, 1962.

[5] A. Loeb, "Direct measurement of cosmological parameters from the cosmic deceleration of extragalactic objects," *Astrophysical Journal*, vol. 499, no. 2, pp. L111–L114, 1998.

[6] S. Qi and T. Lu, "Possible direct measurement of the expansion rate of the universe," http://arxiv.org/abs/1001.3975.

[7] P. S. Corasaniti, D. Huterer, and A. Melchiorri, "Exploring the dark energy redshift desert with the Sandage-Loeb test," *Physical Review D*, vol. 75, no. 6, Article ID 062001, 2007.

[8] J. Zhang, L. Zhang, and X. Zhang, "Sandage-Loeb test for the new agegraphic and Ricci dark energy models," *Physics Letters B*, vol. 691, no. 1, pp. 11–17, 2010.

[9] C. Quercellini, L. Amendola, A. Balbi, P. Cabella, and M. Quartin, "Real-time cosmology," *Physics Reports*, submitted.

[10] H. J. Seo and D. J. Eisenstein, "Probing dark energy with baryonic acoustic oscillations from future large galaxy redshift surveys," *Astrophysical Journal*, vol. 598, no. 2, pp. 720–740, 2003.

[11] G. Bernstein, "Metric tests for curvature from weak lensing and baryon acoustic oscillations," *Astrophysical Journal*, vol. 637, no. 2, pp. 598–607, 2006.

[12] S. Weinberg, *Cosmology*, Oxford University Press, New York, NY, USA, 2008.

[13] S. Weinberg, *Gravitation and Cosmology: Principles and Applications of the General Theory of Relativity*, John Wiley < Sons, New York, NY, USA, 1972.

[14] D. W. Hogg, "Distance measures in cosmology," http://arxiv.org/abs/astro-ph/9905116.

[15] C. Alcock and B. Paczyński, "An evolution free test for non-Zero cosmological constant," *Nature*, vol. 281, no. 5730, pp. 358–359, 1979.

[16] T. Matsubara and Y. Suto, "Cosmological redshift distortion of correlation functions as a probe of the density parameter and the cosmological constant," *Astrophysical Journal*, vol. 470, no. 1, pp. L1–L5, 1996.

[17] W. E. Ballinger, J. A. Peacock, and A. F. Heavens, "Measuring the cosmological constant with redshift surveys," *Monthly Notices of the Royal Astronomical Society*, vol. 282, no. 3, pp. 877–888, 1996.

[18] T. Matsubara and A. S. Szalay, "Apparent clustering of intermediate-redshift galaxies as a probe of dark energy," *Physical Review Letters*, vol. 90, no. 2, Article ID 021302, 4 pages, 2003.

[19] T. Matsubara, "Correlation function in deep redshift space as a cosmological probe," *Astrophysical Journal*, vol. 615, no. 2, pp. 573–585, 2004.

[20] W. J. Percival, S. Cole, D. J. Eisenstein et al., "Measuring the baryon acoustic oscillation scale using the sloan digital sky survey and 2dF galaxy redshift survey," *Monthly Notices of the Royal Astronomical Society*, vol. 381, no. 3, pp. 1053–1066, 2007.

[21] N. Padmanabhan and M. White, "Constraining anisotropic baryon oscillations," *Physical Review D*, vol. 77, no. 12, Article ID 123540, 2008.

[22] http://www.sdss.org/.

[23] R. Jimenez and A. Loeb, "Constraining cosmological parameters based on relative galaxy ages," *Astrophysical Journal*, vol. 573, no. 1, pp. 37–42, 2002.

[24] R. Jimenez, L. Verde, T. Treu, and D. Stern, "Constraints on the equation of state of dark energy and the Hubble constant from stellar ages and the cosmic microwave background," *Astrophysical Journal*, vol. 593, no. 2, pp. 622–629, 2003.

[25] P. J. Mccarthy, D. L. E. Borgne, D. Crampton et al., "Evolved galaxies at $z > 1.5$ from the gemini deep deep survey: the formation epoch of massive stellar systems," *Astrophysical Journal*, vol. 614, no. 1, pp. L9–L12, 2004.

[26] D. Stern, R. Jimenez, L. Verde, M. Kamionkowski, and S. A. Stanford, "Cosmic chronometers: constraining the equation of state of dark energy. I: *H(z)* measurements," *Journal of Cosmology and Astroparticle Physics*, vol. 2010, no. 2, 2010.

[27] D. Stern, R. Jimenez, L. Verde, S. A. Stanford, and M. Kamionkowski, "Cosmic chronometers: constraining the equation of state of dark energy. II. A spectroscopic catalog of red galaxies in galaxy clusters," *Astrophysical Journal, Supplement Series*, vol. 188, no. 1, pp. 280–289, 2010.

[28] J. Simon, L. Verde, and R. Jimenez, "Constraints on the redshift dependence of the dark energy potential," *Physical Review D*, vol. 71, no. 12, Article ID 123001, 2005.

[29] D. P. Carson and R. C. Nichol, "The age-redshift relation for luminous red galaxies in the Sloan Digital Sky Survey," *Monthly Notices of the Royal Astronomical Society*, vol. 408, no. 1, pp. 213–233, 2010.

[30] A. Stockton, M. Kellogg, and S. E. Ridgway, "The nature of the stellar continuum in the radio galaxy 3C 65," *Astrophysical Journal*, vol. 443, no. 2, pp. L69–L72, 1995.

[31] J. Dunlop, J. Peacock, H. Spinrad et al., "A 3.5-Gyr-old galaxy at redshift 1.55," *Nature*, vol. 381, no. 6583, pp. 581–584, 1996.

[32] H. Spinrad, A. Dey, D. Stern et al., "LBDS 53W091: an old, red galaxy at $z = 1.552$," *Astrophysical Journal*, vol. 484, no. 2, pp. 581–601, 1997.

[33] J. S. Alcaniz and J. A. S. Lima, "Dark energy and the epoch of galaxy formation," *Astrophysical Journal*, vol. 550, no. 2, pp. L133–L136, 2001.

[34] R. Jimenez, J. MacDonald, J. S. Dunlop, P. Padoan, and J. A. Peacock, "Synthetic stellar populations: single stellar populations, stellar interior models and primordial protogalaxies," *Monthly Notices of the Royal Astronomical Society*, vol. 349, no. 1, pp. 240–254, 2004.

[35] R. Jimenez, A. C. S. Friaça, J. S. Dunlop, R. J. Terlevich, J. A. Peacock, and L. A. Nolan, "Premature dismissal of high-redshift elliptical galaxies," *Monthly Notices of the Royal Astronomical Society*, vol. 305, no. 1, pp. L16–L20, 1999.

[36] S. M. Crawford, A. L. Ratsimbazafy, C. M. Cress, E. A. Olivier, S.-L. Blyth, and K. J. van der Heyden, "Luminous red galaxies in simulations: cosmic chronometers?" *Monthly Notices of the Royal Astronomical Society*, vol. 406, no. 4, pp. 2569–2577, 2010.

[37] P. J. E. Peebles, "Statistical analysis of catalogs of extragalactic objects. I. Theory," *The Astrophysical Journal*, vol. 185, pp. 413–440, 1973.

[38] X. Xu, M. White, N. Padmanabhan et al., "A new statistic for analyzing baryon acoustic oscillations," *Astrophysical Journal*, vol. 718, no. 2, pp. 1224–1234, 2010.

[39] H. A. Feldman, N. Kaiser, and J. A. Peacock, "Power-spectrum analysis of three-dimensional redshift surveys," *Astrophysical Journal*, vol. 426, no. 1, pp. 23–37, 1994.

[40] W. J. Percival, L. Verde, and J. A. Peacock, "Fourier analysis of luminosity-dependent galaxy clustering," *Monthly Notices of the Royal Astronomical Society*, vol. 347, no. 2, pp. 645–653, 2004.

[41] S. D. Landy and A. S. Szalay, "Bias and variance of angular correlation functions," *Astrophysical Journal*, vol. 412, no. 1, pp. 64–71, 1993.

[42] P. J. E. Peebles and J. T. Yu, "Primeval adiabatic perturbation in an expanding universe," *The Astrophysical Journal*, vol. 162, pp. 815–836, 1970.

[43] W. Hu and N. Sugiyama, "Anisotropies in the cosmic microwave background: an analytic approach," *Astrophysical Journal*, vol. 444, no. 2, pp. 489–506, 1995.

[44] S. Bashinsky and E. Bertschinger, "Dynamics of cosmological perturbations in position space," *Physical Review D*, vol. 65, no. 12, Article ID 123008, 2002.

[45] W. Hu and S. Dodelson, "Cosmic microwave background anisotropies," *Annual Review of Astronomy and Astrophysics*, vol. 40, pp. 171–216, 2002.

[46] G. Hinshaw, D. N. Spergel, L. Verde et al., "First-year Wilkinson Microwave Anisotropy Probe (WMAP) observations: the angular power spectrum," *Astrophysical Journal, Supplement Series*, vol. 148, no. 1, pp. 135–159, 2003.

[47] L. Page, M. R. Nolta, C. Barnes et al., "First-year Wilkinson microwave anisotropy probe (WMAP) observations: interpretation of the TT and TE angular power spectrum peaks," *Astrophysical Journal, Supplement Series*, vol. 148, no. 1, pp. 233–241, 2003.

[48] G. Hinshaw, M. R. Nolta, C. L. Bennett et al., "Three-year Wilkinson Microwave Anisotropyprobe (WMAP) observations: temperature analysis," *Astrophysical Journal, Supplement Series*, vol. 170, no. 2, pp. 288–334, 2007.

[49] M. R. Nolta, J. Dunkley, R. S. Hill et al., "Five-year wilkinson microwave anisotropy probe observations: angular power spectra," *Astrophysical Journal, Supplement Series*, vol. 180, no. 2, pp. 296–305, 2009.

[50] D. Larson, J. Dunkley, G. Hinshaw et al., "Seven-year Wilkinson Microwave Anisotropy Probe (WMAP) observations: power spectra and WMAP-derived parameters," *The Astrophysical Journal Supplement Series*. In press.

[51] D. M. Goldberg and M. A. Strauss, "Determination of the baryon density from large-scale galaxy redshift surveys," *Astrophysical Journal*, vol. 495, no. 1, pp. 29–43, 1998.

[52] A. Meiksin, M. White, and J. A. Peacock, "Baryonic signatures in large-scale structure," *Monthly Notices of the Royal Astronomical Society*, vol. 304, no. 4, pp. 851–864, 1999.

[53] D. J. Eisenstein, I. Zehavi, D. W. Hogg et al., "Detection of the baryon acoustic peak in the large-scale correlation function of SDSS luminous red galaxies," *Astrophysical Journal*, vol. 633, no. 2, pp. 560–574, 2005.

[54] C. Blake and K. Glazebrook, "Probing dark energy using baryonic oscillations in the galaxy power spectrum as a cosmological ruler," *Astrophysical Journal*, vol. 594, no. 2, pp. 665–673, 2003.

[55] H. J. Seo and D. J. Eisenstein, "Baryonic acoustic oscillations in simulated galaxy redshift surveys," *Astrophysical Journal*, vol. 633, no. 2, pp. 575–588, 2005.

[56] H. J. Seo and D. J. Eisenstein, "Improved forecasts for the baryon acoustic oscillations and cosmological distance scale," *Astrophysical Journal*, vol. 665, no. 1, pp. 14–24, 2007.

[57] M. Davis and P. J. E. Peebles, "A survey of galaxy redshifts. V - The two-point position and velocity correlations," *The Astrophysical Journal*, vol. 267, pp. 465–482, 1983.

[58] N. Kaiser, "Clustering in real space and in redshift space," *Monthly Notices of the Royal Astronomical Society*, vol. 227, pp. 1–21, 1987.

[59] H. Magira, Y. P. Jing, and Y. Suto, "Cosmological redshift-space distortion on clustering of high-redshift objects: correction for nonlinear effects in the power spectrum and tests with N-body simulations," *Astrophysical Journal*, vol. 528, no. 1, pp. 30–50, 2000.

[60] N. Kaiser, "On the spatial correlations of Abell clusters," *The Astrophysical Journal*, vol. 284, pp. L9–L12, 1984.

[61] L. Hui, E. Gaztañaga, and M. LoVerde, "Anisotropic magnification distortion of the 3D galaxy correlation. I. Real space," *Physical Review D*, vol. 76, no. 10, Article ID 103502, 2007.

[62] L. Hui, E. Gaztañaga, and M. LoVerde, "Anisotropic magnification distortion of the 3D galaxy correlation. II. Fourier and redshift space," *Physical Review D*, vol. 77, no. 6, Article ID 063526, 2008.

[63] T. Okumura, T. Matsubara, D. J. Eisenstein et al., "Large-scale anisotropic correlation function of SPSS luminous red galaxies," *Astrophysical Journal*, vol. 676, no. 2, pp. 889–898, 2008.

[64] E. Gaztañaga, A. Cabré, and L. Hui, "Clustering of luminous red galaxies - IV. Baryon acoustic peak in the line-of-sight direction and a direct measurement of $H(z)$," *Monthly Notices of the Royal Astronomical Society*, vol. 399, no. 3, pp. 1663–1680, 2009.

[65] E. Komatsu, J. Dunkley, M. R. Nolta et al., "Five-year wilkinson microwave anisotropy probe observations: cosmological interpretation," *Astrophysical Journal, Supplement Series*, vol. 180, no. 2, pp. 330–376, 2009.

[66] J. Miralda-Escude, "Comment on the claimed radial BAO detection by Gaztanaga et al," http://arxiv.org/abs/0901.1219.

[67] E. A. Kazin, M. R. Blanton, R. Scoccimarro, C. K. McBride, and A. A. Berlind, "Regarding the line-of-sight baryonic acoustic feature in the Sloan Digital Sky Survey and baryon Oscillation Spectroscopic Survey luminous red galaxy samples," *Astrophysical Journal*, vol. 719, no. 2, pp. 1032–1044, 2010.

[68] A. R. Liddle, "Statistical methods for cosmological parameter selection and estimation," *Annual Review of Nuclear and Particle Science*, vol. 59, pp. 95–114, 2009.

[69] H. J. Tian, M. C. Neyrinck, T. Budavari, and A. S. Szalay, "Redshift-space enhancement of line-of-sight baryon acoustic oscillations in the SDSS main-galaxy sample," *The Astrophysical Journal*, submitted.

[70] A. Cabre and E. Gaztanaga, "Have Baryonic Acoustic Oscillations in the galaxy distribution really been measured?" *Monthly Notices of the Royal Astronomical Society*, submitted.

[71] J. Dunkley, E. Komatsu, M. R. Nolta et al., "Five-year wilkinson microwave anisotropy probe observations: likelihoods and parameters from the WMAP data," *Astrophysical Journal, Supplement Series*, vol. 180, no. 2, pp. 306–329, 2009.

[72] A. G. Riess, L. Macri, S. Casertano et al., "A redetermination of the hubble constant with the hubble space telescope from a differential distance ladder," *Astrophysical Journal*, vol. 699, no. 1, pp. 539–563, 2009.

[73] D. G. Figueroa, L. Verde, and R. Jimenez, "Improved cosmological parameter constraints from CMB and $H(z)$ data," *Journal of Cosmology and Astroparticle Physics*, vol. 2008, no. 10, article no. 038, 2008.

[74] B. A. Reid, L. Verde, R. Jimenez, and O. Mena, "Robust neutrino constraints by combining low redshift observations with the CMB," *Journal of Cosmology and Astroparticle Physics*, vol. 2010, no. 1, article no. 003, 2010.

[75] Y. I. Izotov, T. X. Thuan, and G. Stasińska, "The primordial abundance of ^{4}He: a self-consistent empirical analysis of systematic effects in a large sample of low-metallicity H II regions," *Astrophysical Journal*, vol. 662, no. 1, pp. 15–38, 2007.

[76] F. Iocco, G. Mangano, G. Miele, O. Pisanti, and P. D. Serpico, "Primordial nucleosynthesis: from precision cosmology to fundamental physics," *Physics Reports*, vol. 472, no. 1–6, pp. 1–76, 2009.

[77] C. Clarkson, M. Cortês, and B. Bassett, "Dynamical dark energy or simply cosmic curvature?" *Journal of Cosmology and Astroparticle Physics*, vol. 2007, no. 8, article 011, 2007.

[78] M. Vardanyan, R. Trotta, and J. Silk, "How flat can you get? A model comparison perspective on the curvature of the Universe," *Monthly Notices of the Royal Astronomical Society*, vol. 397, no. 1, pp. 431–444, 2009.

[79] HU. Zhan, L. Knox, and J. A. Tyson, "Distance, growth factor, and dark energy constraints from photometric baryon acoustic oscillation and weak lensing measurements," *Astrophysical Journal*, vol. 690, no. 1, pp. 923–936, 2009.

[80] E. Gaztañaga, R. Miquel, and E. Sánchez, "First cosmological constraints on dark energy from the radial baryon acoustic scale," *Physical Review Letters*, vol. 103, no. 9, Article ID 091302, 2009.

[81] Z. L. Yi and T. J. Zhang, "Constraints on holographic dark energy models using the differential ages of passively evolving galaxies," *Modern Physics Letters A*, vol. 22, no. 1, pp. 41–53, 2007.

[82] L. Samushia and B. Ratra, "Cosmological constraints from Hubble parameter versus redshift data," *Astrophysical Journal*, vol. 650, no. 1, pp. L5–L8, 2006.

[83] F. C. Carvalho, E. M. Santos, J. S. Alcaniz, and J. Santos, "Cosmological constraints from the Hubble parameter on *f(R)* cosmologies," *Journal of Cosmology and Astroparticle Physics*, vol. 2008, no. 9, article no. 008, 2008.

[84] L. Xu and Y. Wang, "Observational constraints to ricci dark energy model by using: SN, BAO, OHD, fgas data sets," *Journal of Cosmology and Astroparticle Physics*, vol. 2010, no. 6, 2010.

[85] I. Durán, D. Pavón, and W. Zimdahl, "Observational constraints on a holographic, interacting dark energy model," *Journal of Cosmology and Astroparticle Physics*, vol. 2010, no. 7, article 018, 2010.

[86] V. Sahni, A. Shafieloo, and A. A. Starobinsky, "Two new diagnostics of dark energy," *Physical Review D*, vol. 78, no. 10, Article ID 103502, 2008.

[87] C. Zunckel and C. Clarkson, "Consistency tests for the cosmological constant," *Physical Review Letters*, vol. 101, no. 18, Article ID 181301, 2008.

[88] C. Clarkson, B. Bassett, and T. H. C. Lu, "A general test of the copernican principle," *Physical Review Letters*, vol. 101, no. 1, Article ID 011301, 2008.

[89] A. Shafieloo and C. Clarkson, "Model independent tests of the standard cosmological model," *Physical Review D*, vol. 81, no. 8, Article ID 083537, 2010.

[90] N. Pan, Y. Gong, Y. Chen, and Z. -H. Zhu, "Improved cosmological constraints on the curvature and equation of state of dark energy," *Classical and Quantum Gravity*, vol. 27, no. 15, Article ID 155015, 2010.

[91] Z. X. Zhai, H. Y. Wan, and T. J. Zhang, "Cosmological constraints from radial baryon acoustic oscillation measurements and observational Hubble data," *Physics Letters B*, vol. 689, no. 1, pp. 8–13, 2010.

[92] L. Verde, "Statistical methods in cosmology," *Lecture Notes in Physics*, vol. 800, pp. 147–177, 2010.

[93] A. G. Riess, L. G. Sirolger, J. Tonry et al., "Type Ia supernova discoveries at $z > 1$ from the hubble space telescope: evidence for past deceleration and constraints on dark energy evolution," *Astrophysical Journal*, vol. 607, no. 2 I, pp. 665–687, 2004.

[94] C. Ma and T.-J. Zhang, "Power of observational Hubble parameter data: a figure of merit exploration,"*Astrophysical Journal*. In press.

[95] http://www.physics.princeton.edu/act/index.html.

[96] N. Bentez, E. Gaztanaga, R. Miquel et al., "Measuring baryon acoustic oscillations along the line of sight with photometric redshifts: the PAU survey," *The Astrophysical Journal*, vol. 691, pp. 241–260, 2009.

[97] P. Arnalte-Mur, A. Fernández-Soto, V. J. Martínez, E. Saar, P. Heinämäki, and I. Suhhonenko, "Recovering the real-space correlation function from photometric redshift surveys," *Monthly Notices of the Royal Astronomical Society*, vol. 394, no. 3, pp. 1631–1639, 2009.

[98] D. Roig, L. Verde, J. Miralda-Escudé, R. Jimenez, and C. Peña-Garay, "Photo-*z* optimization for measurements of the BAO radial scale," *Journal of Cosmology and Astroparticle Physics*, vol. 2009, no. 4, article 008, 2009.

[99] http://wigglez.swin.edu.au/.

[100] M. J. Drinkwater, R. J. Jurek, C. Blake et al., "The WiggleZ Dark Energy Survey: survey design and first data release," *Monthly Notices of the Royal Astronomical Society*, vol. 401, no. 3, pp. 1429–1452, 2010.

[101] http://www.sdss3.org/.

[102] P. McDonald and D. J. Eisenstein, "Dark energy and curvature from a future baryonic acoustic oscillation survey using the Lyman-α forest," *Physical Review D*, vol. 76, no. 6, Article ID 063009, 2007.

[103] M. L. Norman, P. Paschos, and R. Harkness, "Baryon acoustic oscillations in the Lyman alpha forest," *Journal of Physics: Conference Series*, vol. 180, no. 1, 2009.

[104] M. White, A. Pope, J. Carlson et al., "Particle mesh simulations of the Lyα Forest and the signature of baryon acoustic oscillations in the intergalactic medium," *Astrophysical Journal*, vol. 713, no. 1, pp. 383–393, 2010.

[105] A. Cimatti, M. Robberto, C. Baugh et al., "SPACE: the spectroscopic all-sky cosmic explorer," *Experimental Astronomy*, vol. 23, no. 1, pp. 39–66, 2009.

[106] "Euclid assessment study report for the ESA Cosmic Visions," http://arxiv.org/abs/0912.0914.

[107] Y. Wang, W. Percival, A. Cimatti et al., "Designing a space-based galaxy redshift survey to probe dark energy," *Monthly Notices of the Royal Astronomical Society*, vol. 409, no. 2, pp. 737–749, 2010.

[108] R. Barkana and A. Loeb, "Probing the epoch of early baryonic infall through 21-cm fluctuations," *Monthly Notices of the Royal Astronomical Society*, vol. 363, pp. L36–L40, 2005.

[109] X.-C. Mao and X.-P. Wu, "Signatures of the baryon acoustic oscillations on 21 cm emission background," *Astrophysical Journal*, vol. 673, no. 2, pp. L107–L110, 2008.

[110] H. -J. Seo, S. Dodelson, J. Marriner et al., "A ground-based 21 cm baryon acoustic oscillation survey," *Astrophysical Journal*, vol. 721, no. 1, pp. 164–173, 2010.

[111] M. Shoji, D. Jeong, and E. Komatsu, "Extracting angular diameter distance and expansion rate of the universe from two-dimensional galaxy power spectrum at high redshifts: Baryon acoustic oscillation fitting versus full modeling," *The Astrophysical Journal*, vol. 693, pp. 1404–1416, 2009.